

Mitigation of electrical hazards on the metallic pipelines due to the HVOHTLs based on different intelligent controllers

ISSN 1751-8822

Received on 26th May 2020

Revised 10th November 2020

Accepted on 14th December 2020

E-First on 4th March 2021

doi: 10.1049/iet-smt.2020.0218

www.ietdl.org

Mostafa Al-Gabalawy¹ ✉, Mohamed A. Mostafa², Abdel Salam Hamza³

¹Electrical Power Engineering and Automatic Control Department, Pyramids Higher Institute for Engineering and Technology, Egypt

²Electrical Power and Machines Department, MUST University, 6th October, Cairo, Egypt

³Electrical Power and Machines Department, Benha University, Shoubra, Cairo, Egypt

✉ E-mail: mostafagalawy@gmail.com

Abstract: Many catastrophes may occur due to the interference between the metallic pipeline and the high voltage overhead transmission lines (HVOHTLs). These problems exist due to the neighbouring between the HVOHTLs and the other infrastructures. Many types of research cover cathodic protection points, detailed description for the production of the AC voltage, and preliminary mitigation ways. Mainly potassium hydroxide-polarisation cells (KOH-PCs) have been applied to discharge this voltage to the soil. Based on the KOH-PCs electrical model introduced previously, this study investigates a novel mitigation technique, where the discharged AC voltage converts to DC voltage that is proper for the cathodic protection for the metallic pipelines. An integrated system consists of power electronic circuits and distributed intelligent controllers designed to discharge the AC induced voltage and use in the cathodic protection for the pipelines. Different controllers such as the artificial neural network, a fuzzy logic controller, and adaptive neuro-fuzzy inference system controllers have been implemented. Two key performance indicators have been investigated to show the superiority of these controllers, where the total discharged energy per annum (DE_{year}) from the pipeline to the soil, and the total saved per year (SE_{year}).

1 Introduction

The corrosion phenomenon represents the most important concerns that affect the lifetime of buried pipelines. Besides, the corrosion rate may accelerate if the electromagnetic interference between the neighbouring transmission line and the pipeline exists [1]. Many mechanisms illustrate the effect of the interference on the buried pipeline outcomes that induced voltage on it. These mechanisms rely upon the form of coupling (capacitive inductive and conductive) among the pipeline and the transmission line [2]. Conductive coupling generates through the ground voltage rise produced by discharging a very high amount of current into the soil at power system constructions, particularly at the grounding systems of high voltage overhead transmission lines. The conductive coupling is one of the main interests during power system faults, especially when the metallic pipelines are located close to the high voltage transmission line [3]. Commonly, inductive coupling is produced through magnetic fields. The transmission line carrying a high level of current by their conductors generates strong magnetic fields in the neighbouring area. The generated magnetic field nearby the high voltage transmission lines induces a voltage in the surrounding metallic structures coupled with this magnetic field. This coupling is influenced by different factors, such as the transmission line's current, the parallelism length, and the distance between the transmission line and metallic constructions [4]. Over the past decades, various corrosion control methods for the buried pipeline were applied as coating and cathodic protection (CP). Buried pipelines are usually protected from corrosion by providing a good coating with CP [5]. NACE approved the CP guidelines for the buried pipeline is -0.85 V (related to Cu/CuSO₄ electrode, CSE) with AC density <20 A/m² [6, 7]. Almost, the AC interference affects CP's effectiveness and deviates the DC-CP potential of the buried pipeline from the desired value [8].

The artificial intelligence (AI) based techniques have been identified as a preferred solution for the computation of AC induced voltages. Among various AI-based techniques, an adaptive neuro-fuzzy inference system (ANFIS) is the most broadly employed method for modelling the induced voltages. In [9], a

hybrid prediction system composed of an ANFIS and a backtracking search algorithm (BSA) was formed to predict the induced voltage on mitigated and unmitigated pipelines reliably. In the ANFIS learning process, the BSA was considered one of the newly developed metaheuristic optimisation algorithms for tuning the membership functions to achieve a lower prediction error. An adaptive neuro fuzzy-based model was designed to examine the impact of the microstructural parameter variation on the pipeline's pitting corrosion performance. The proposed model would be a useful means to manage the metal's approval/refusal on a market scale [10]. In [11], the pipeline coating defect effects on the induced voltage were introduced. The induced AC voltages mitigation was presented based on the least square method for inserting the suitable number of polarisation cells along the pipeline. A methodology was introduced to predict the buried pipeline's external corrosion rate based on the combination of the soil parameters. This method provided the inspection corrosion rate data and also focused the efforts towards optimising the security and the continuity of the service [12]. In [13], the impressed cathodic protection (ICCP) anode locations on ships were selected based on minimising the underwater electric field. For predicting positions of the ICCP anodes, multiple linear regression analysis and artificial neural network (ANN) methods were applied. The results showed that the ANN was more effective than the multiple linear regression model to predict ICCP-anode and underwater electric field position. Some researchers had attempted to introduce the fuzzy mathematics concept into safety assessment methods of process industries to effectively deal with uncertainty (i.e. incomplete and imprecise data). An analytic model based on the means of the type-2 fuzzy logic controller (T2-FLC) was developed to estimate the corrosion failure likelihood for oil and gas pipelines [14]. In [15], a methodology was proposed to predict the buried pipes corrosion rates based on the combination of the measurement of six soil parameters (moisture content, pH, resistivity, redox potential, sulphate, and chloride concentrations) to decrease the amount of examination corrosion rate data. The technique was based on coupling a fuzzy logic expert system (FLES) within-site investigation data that provides for tremendous control of the pipe corrosion rate. The output of the FLES displays

the level of soil corrosivity that may be non-destructive or extra destructive. In [16], an analytic model for assessing corrosion failure likelihood of oil and gas pipelines had been developed using the fuzzy logic approach. Besides, the fuzzy logic system was used to analyse corrosion thinning likelihood and corrosion cracking likelihood. The proposed model was intended to examine the pipeline failure probability by fuzzy fault tree analysis (FFTA) with expert experience. The proposed FFTA structure was used to make decisions related to oil and gas pipelines 'risk management when struck by multiple natural hazards [17]. A modern PLC-based fuzzy proportional–integral–derivative (PID) controller is planned to automatically regulate the petroleum product flow rate by checking the various pressure signals range in the long transmitting concrete pipes. The real-time data of pressure and flow are monitored by a SCADA screen used to provide instantaneous trends using data logging. Besides, implementing a PLC-based fuzzy-PID controller was developed to increase the control valves operation to avoid environmental interruptions like leakage or damage/explosion in the pipeline transport system [18]. In [19], an AI-based approach was implemented to examine the electromagnetic interference problems between high voltage overhead power lines and nearby buried metallic pipelines. In the case of various geometries and multilayer soil structures, the executed ANN technique assessed the inductive coupling form, which represented the electromagnetic interference problem. Two-hybrid risk assessment systems have been developed, combining the FIS, ANNs, and expert risk assessment methodology to accomplish risk assessment [20]. They concluded that the corrosion growth rate increased when the metal loss was increased and decreased when the pipeline's CP was carefully maintained. Besides, the fuzzy logic model was used in the prediction of pipeline failure [21]. In [22], the methodology was presented to estimate the probability of pipeline failure of CO₂ transporting pipeline based on the combination of fault tree analysis (FTA) with fuzzy logic. The combination of FTA with fuzzy logic would help in artificially generating the unavailable data. In [23], the author established a new fuzzy inference system (FIS) for pipeline risk

assessment. Among various AI-based methods, ANNs were the most broadly applied methods for calculating the induced voltages and evaluating the magnetic vector potential for different constructive geometries of a specific interference problem [24]. The multilayer perceptron (MLP) with the error backpropagation training method as an effective feed-forward class ANN was executed in [25] to predict the induced voltages on a buried pipeline, placed in the electromagnetic field triggered by high voltage transmission lines during the single-phase to ground fault conditions. For this investigation, different parameters were considered as inputs for ANN. These parameters involve the soil resistivity, the distance between the transmission line and the buried pipeline, the magnitude of the fault current, and the connection of the mitigation unit along the pipeline. In [26], an ANN design was approved to predict total voltage on mitigated pipelines due to the impact of inductive and conductive AC interference under fault conditions. Besides, the developed ANN predicted the mitigated voltage of the pipeline under different conditions such as soil resistivities, fault currents, and separation distances. The historical operating parameters were used for establishing the time-dependent corrosion defect depth growth of corroded pipelines based on machine learning tools. The machine learning relies on feed-forward subspace clustered neural network (NN) and particle swarm optimisation in the evaluation of the corrosion defect depth to estimate the integrity of the pipelines at discrete localities [27]. Optimisation of an ANN modelling methodology for the reliability evaluation of corroding natural gas pipelines was introduced [28]. In [29], an improved flower pollination algorithm was proposed by combining the global iterative chaotic map with a comprehensive opposition learning approach to efficiently optimise the backpropagation neural network's initial weights and thresholds. This will promote intelligent examination of natural gas pipelines defects as well as recognise the state of pipeline normal state; pit defect, and scratch defect. Table 1 summarises the recent works on corrosion control applications in terms of controller type. This paper introduces the implementation of many intelligent controllers to discharge the AC induced voltage from the pipeline to the soil due to the interference with the transmission lines. Additionally, this paper introduces a design for a circuit to convert the AC voltage to DC voltage proper for CP. The total delivered from the utility to CP is reduced due to this conversion. Moreover, two novel key performance indicators (KPIs) have been represented to compare between the applied control algorithms; FLC, ANN, and ANFIS. The first one demonstrates the total saved energy from the utility per year, while the second describes the total discharged energy to the soil per year. The rest of the paper is organised as follows: Section 2 introduces the problem statement with the basic structure for AC corrosion control. Section 3 describes the proposed solution. Furthermore, details of the proposed algorithms are introduced in Section 4. The implementation of the proposed algorithms for the main and distributed ICCP stations is introduced in Section 5. Furthermore, the results of the proposed model and a comparative performance evaluation for different controllers with various models of potassium hydroxide (KOH), PC-25, and PC-50 are introduced in Section 6. Finally, conclusions and possible future work are given in Section 7.

Table 1 Summary of the reviewed corrosion research works and applications

References	Tool	Objective
Aghay <i>et al.</i> (2019) [6]	ANFIS	prediction of metallic conductor voltage
Ahmed (2018) [7]		estimation of coating defects
Roya and Bhardwajb [10]		estimation of the pitting corrosion
Yuji <i>et al.</i> (2002) [8]	FLC	predicting pipeline external corrosion rate'
Roya and Bhardwajb (2018) [10] and Ahmed (2018) [11]		estimation of corrosion failure
Kim and Seok (2018) [13], and Qi and Wei (2016) [16]		pipeline risk assessment
Victoria <i>et al.</i> (2018) [15]		estimation of failure probability
Priyanka <i>et al.</i> [18]		adjust the flow rate of the petroleum products
Aghay <i>et al.</i> (2019) [9]	ANN	optimising anode location in an ICCP system
Biezma and Agudo (2018) [12]		studying inductive coupling between overhead power lines and nearby metallic pipelines
Dipak and Barnali (2017) [14]		they are predicting the condition of offshore oil and gas pipelines.
Pavanaditya <i>et al.</i> (2018) [17], and Priyanka <i>et al.</i> (2018) [18]		studying the electromagnetic interference
Levente <i>et al.</i> (2016) [19] and Wu (2015) [20]		prediction of voltages on mitigated pipelines
Xiaobin <i>et al.</i> [27]		estimation of the corrosion defect depth

2 Problem statement

This section provides a detailed description of induced AC voltage causes on the pipeline due to transmission line interference. Besides, the electrical modelling of the impressed current system and the polarisation cell is illustrated.

2.1 Mechanisms of induced AC voltage

As discussed in [30], three forms discuss the reasons for the induced voltages produced on the pipeline. These forms can be summarised, dependently on the type of the coupling between the pipeline and transmission line, into capacitive, inductive, and conductive. In this study, only the inductive form is introduced because the pipeline is buried at depth in the soil. This form occurs when AC flowing in the transmission line produces a magnetic

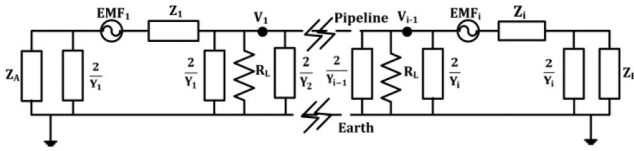


Fig. 1 Equivalent circuit of a pipeline multi-sections

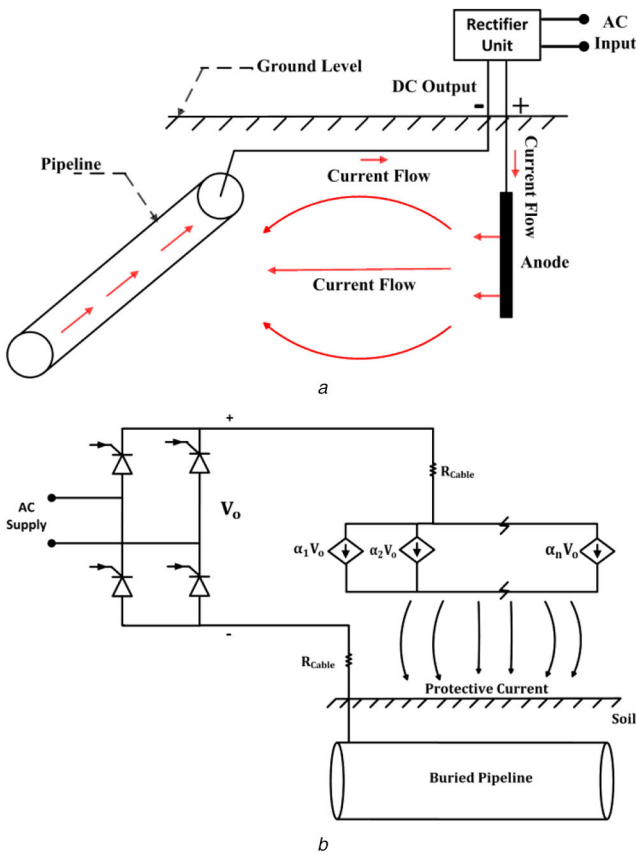


Fig. 2 The model of impressed current cathodic protection (ICCP) system (a) The layout of ICCP system, (b) Diagram of an impressed-current CP system for a buried pipeline

field around the transmission lines, which induced voltages on the nearby buried pipeline. The induced voltage produced on the pipeline is dependent on the transmission line's current. This voltage may be serious for the pipeline's CP performance due to AC corrosion [30]. There are different techniques to calculate the induced voltage on the pipeline [31]. This study presents the chosen method [32, 33], which has high consistency in the simulation results.

The AC flowing in the overhead transmission lines causes a magnetic field, which induces the pipeline's voltage. The induced voltage is calculated based on the lossy transmission line modelling. In this model, the pipeline is divided into several segments; each segment has the equivalent impedance and admittance of the pipeline related to the earth. Besides, the induced AC voltage at each section is calculated based on the driving electric field (E_i), the impedance, and admittance of the pipeline related to the earth per unit length (Z and Y), respectively, and also the uniform grounding parameters such as the soil resistance and pipeline coating resistance, which represents as (R_L). Fig. 1 shows the equivalent electrical circuit of the pipeline [32]. Usually, the pipeline voltage at each segment can be calculated as (1) [33], and the details of the parameters calculations are discussed in [34].

The induced AC voltage produced at each π -pipeline section is estimated as follows:

$$V_i = \frac{E_i}{\gamma} \left\{ -\frac{Z_A}{Z_A + Z_C} e^{-\gamma x} + \frac{Z_B}{Z_B + Z_C} e^{-\gamma(L_p - x)} \right\} \quad (1)$$

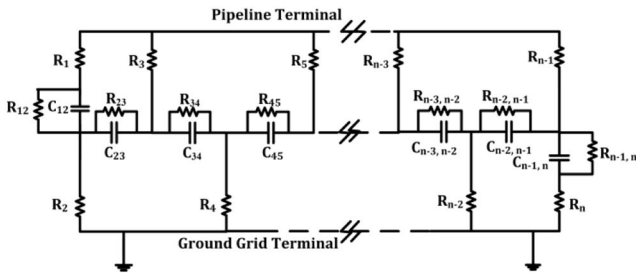
where i is an index that relates to each segment of the pipeline, E_i represents the driving electric field force per unit length (V/m), γ is the propagation constant that equals $\sqrt{ZY}(\text{m}^{-1})$, Z_C is the characteristic impedance, that equals $\sqrt{Z/Y}(\Omega)$, Z and Y are the impedance and admittance of the pipeline to ground per unit length, respectively, Z_A and Z_B are the equivalent impedance of buried pipeline per unit length on the left and right sides, respectively (Ω), L_p is the length of each section (m), and x is a variable distance (m).

2.2 AC corrosion control

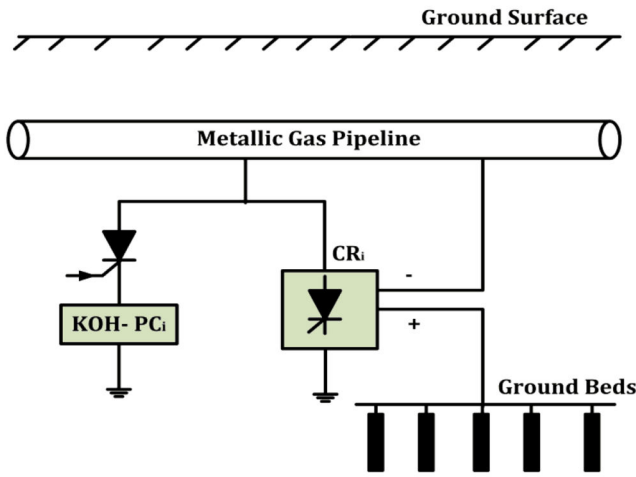
The induced AC voltage is produced on the buried pipeline, which may result from nearby transmission lines to the pipeline. This voltage may result in AC on the pipeline, which causes pipeline corrosion. This corrosion will occur if the corrosion current exceeds the injected DC by the CP unit [35]. The rate of corrosion is dependent on the AC density so that the increase of AC density will be accelerated the corrosion rate. For solving this problem, there are two methods applied to prevent pipeline corrosion, namely coatings and CP. It is essential to combine coatings and CP to reduce AC corrosion probability on the pipeline. The principle of CP is to deliver an appropriate direct current to the pipeline to increase the DC voltage of the protected pipeline until the corrosion is mitigated [36]. The CP means on the pipeline can be classified into two types; in the first type (ICCP), an external DC power source is used as in Fig. 2. While in the second type, a sacrificial anode cathodic protection (SACP) is used [37]. Generally, the ICCP method is the most effective way to protect the long transmission pipelines, especially due to flexibility in voltage and current adjustments to the pipeline [38]. In this method, the impressed current depends on two mechanisms; the first one is the variation of the external resistance of the CP circuit to keep the CP potential at the desired limit. The other mechanism is the variation of the output current from the impressed current unit. The amount of DC injected into the pipeline to overcome the pipeline's corrosion is dependent on several factors [35]. These factors are the protected pipeline area, the electrolyte type between the pipeline and ground anodes bed, the metal type of the anodes, and the type of pipeline's coating. The selection of the coating materials very significant to reduce the required DC significantly as it acts as an insulation medium between the pipeline and the surrounding environment. The most vital factor is the soil resistivity that changes with weather or environmental conditions since the injected DC is also varied with these conditions either increases or decreases to achieve constant DC voltage along the pipeline. Either manual or automatic adjustment achieves the required DC-CP potential on the buried pipeline. The two mechanisms 'overall purpose is to maintain the DC voltage within the safe limits' (-0.85 to -1.5 V).

The conventional ICCP system is illustrated in detail as shown in Fig. 2a, where the DC is delivered into the pipeline from an external DC source (usually a power rectifier). The positive side of this source is solidly connected to a group of graphite anodes. These anodes deliver a DC through the soil to the pipeline, where the negative side of the power rectifier is connected to the pipeline. Fig. 2b shows the schematic diagram of an impressed system with a single-phase controlled rectifier circuit. The negative terminal of the fully controlled single-phase rectifier circuit is attached to the pipeline. The positive end is linked to a series of anodes bed. Each anode is defined by a dependent source of current, which depends on the DC voltage output value. Each anode is connected in parallel, and the total current is $\sum_n^a V_o$, which represents the sum of the drawn current from each anode.

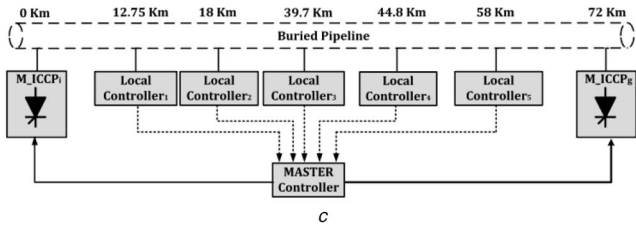
In this study, there are two ICCP stations at both ends of the pipeline, where the transformer rectifier is used to step down the AC input from a grid to normal voltage and then rectified this by the controlled rectifier circuit. Hence, along the actual Fayoum gas pipeline, there are two impressed current system units. Additionally, this line has five potassium hydroxide-polarisation cells (KOH-PCs) that installed the points of the AC voltage peak points.



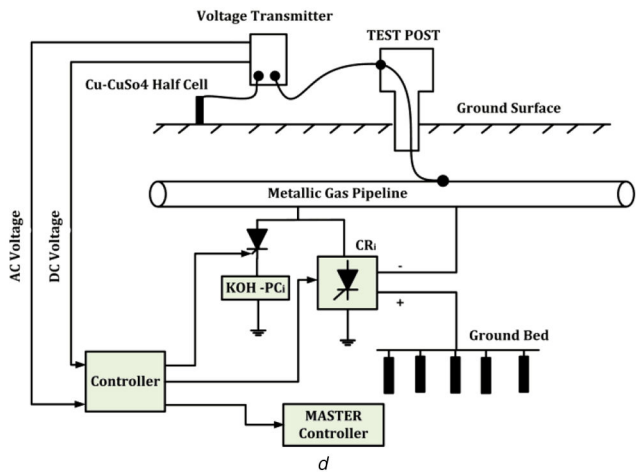
a



b



c



d

Fig. 3 Schematic representation of the proposed model (a) Equivalent circuit of the KOH-PCs'components, (b) Detailed scheme description for the suggested model, (c) The complete configuration for the installed distributed controller, main ICCP stations, and main controller for the pipeline, (d) Detailed layout of the proposed model-based different controller applied to the system

The required DC for CP strongly depends on several factors such as quality of coating materials, soil conductivity, the total protected area of the pipeline, the variation of the DC-CP potential, which can be illustrated by (2) [39]:

$$i_i = -\sigma_l \cdot \nabla \phi_l \quad (2)$$

where i_i is the soil current density (A/m^2), σ_l is the conductivity of the soil (S/m), and ϕ_l is the DC potential from the pipeline to anode bed (Volt).

The default insulation limit for all buried pipeline boundaries is defined as:

$$\nabla \cdot i_i = 0. \quad (3)$$

3 Proposed solution

As described in the above sections, the pipeline of Fayoum Gas Company has mainly two ICCP units and five KOH-PCs. Moreover, the electrical circuits of ICCP and KOH-PC are shown in Figs. 3a and b, respectively [34]. An additional controlled AC switch (thyristor) has been installed between the pipeline and the KOH-PC. In parallel with each cell, a distributed controlled rectifier circuit (DCRC) is installed. The positive side of this circuit is connected to a small group of graphite anodes, while the negative side of it is connected to the pipeline's local point, as shown in Fig. 3b. Fig. 3c shows that the complete configuration for the installed distributed controller, main ICCP stations, and central controller for the pipeline. A comprehensive monitoring system has been applied, where both AC and DC voltages of the selected five points are received. These signals are then processed through a master controller, where this controller delivers the fire angle pulses to the thyristors of central ICCP units, KOH-PC AC switch, and the parallel control rectifier circuit, as in Fig. 3d. Simultaneously, the flowchart is presented in Fig. 4, which summarises the implementation process to enhance the CP performance and mitigate the induced AC voltage along the pipeline for protecting the pipeline against corrosion. Firstly, the pipeline and transmission line data are collected, then the measurement of the soil resistivity is carried out. The induced AC and DC voltages along the pipeline is measured or calculated. This voltage is compared with the voltage limit value of 15 V for AC voltage and between -0.85 and -1.5 V for DC voltage. If both AC and DC voltages are within threshold limits, no action will be achieved by the control system. If both AC and DC voltages at any point are more than the limit value, some procedures are recommended to reach these voltages to limit set. These procedures incorporate the decrease of the KOH-PC's firing angle, which means dissipating the induced AC voltage into the soil is increased. On the other hand, the firing angle of the controlled rectifier is increased, which means the distributed ICCP will be out of service, in addition to the main ICCP until the CP potential and induced AC voltage reaches the desired limit. If the AC voltage is greater than the threshold value and DC voltages at any point are less than the limit value. Inserting a KOH-PC should be carried out to reduce the induced voltage as well as both distributed, and the main ICCP should inject to increase the CP potential. If the AC voltage is less than the threshold value and DC voltages at any point are more than the limit value. In this case, there is no need to connect any KOH-PC, in addition to the injected current from main ICCP stations is reduced. Furthermore, there is no need to connect any distributed impressed current. If the AC and DC voltages at any point are less than the limit value, some procedures are recommended to increase the DC voltage to the limit value. In this case, the increase of the KOH-PC's firing angle is carried out to decrease the dissipating of the induced AC voltage to the soil and increase its utilisation in the process of rectification. Besides, the controlled rectifier's firing angle decreases to raise the injected current on the pipeline from the distributed ICCP. The impressed current from the main ICCP increases by decreasing the central controller rectifier circuit's firing angle.

4 Proposed algorithms

In this study, ANN, FLC, and ANFIS are applied to control either the discharging energy into the soil or the injected energy on the pipeline. The annual saving energy (SE_{year}) is selected as a KPI that represents either the discharged energy from the pipeline into the soil or the converted energy to the pipeline in DC CP voltage form. This KPI shows that the delivered energy from the external

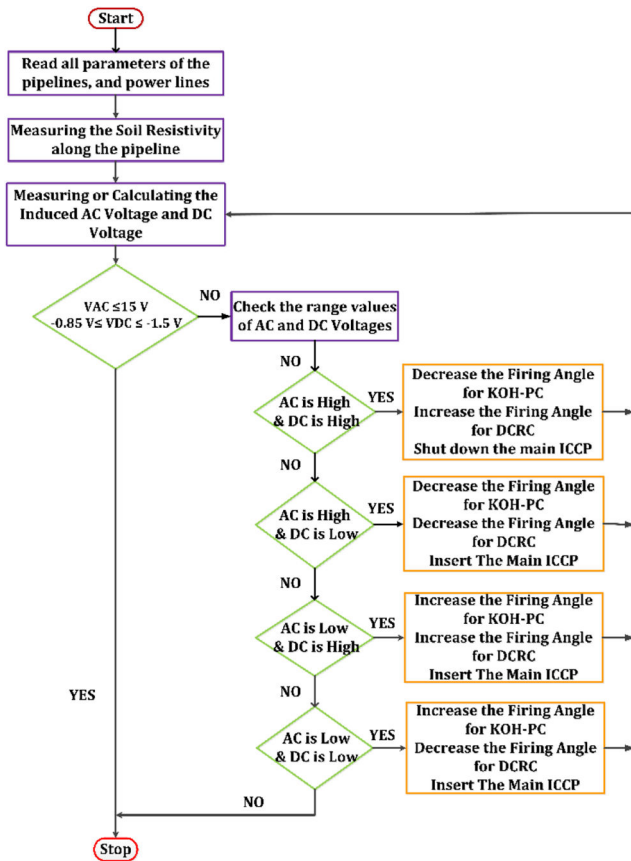


Fig. 4 Control algorithm of eliminating the AC induced voltage maximising the DC-CP voltage of the pipeline

CP stations to the pipeline should be minimised, and also the discharged energy from the pipeline should be maximised. The following sections describe the applied control algorithms to achieve the highest SE_{year} .

4.1 Fuzzy logic controller

FLC mimics human decision making, where it allows for analysis of complicated system structures in which linguistic expressions are used instead of numerical variables for modelling the system. It has increasingly been used in various fields such as economics, image processing, power engineering, systems engineering, optimisation, industrial automation, and varied purpose robotics [40–42]. Fuzzy modelling is basically a rule-based method, which is also described as a fuzzy inference framework. A typical fuzzy logic system consists of four major parts, as illustrated in Fig. 5a, fuzzification, fuzzy rule base, fuzzy inference, and defuzzification.

Firstly, the variables for input and output are determined, then fuzzy sets are defined for these variables. Membership functions have been built to show the relationship between the inputs and the outputs. There are various types of membership functions, including triangular, Gaussian, trapezoidal, and so on. Since membership type functions impact the FLC architecture, it is necessary to choose carefully. The fuzzy IF-THEN rules are generated to relate variables for input and output. Fifth, the mechanism of inference is set. The two most popular forms of fuzzy interface system (FIS) are the Mamdani, and the Sugeno, where Sugeno's output is linear or constant, but Mamdani's output consists of membership functions that might be trapezoidal, triangular etc. Sugeno is also trained using the data set, but Mamdani does not need a data set and relies on expert knowledge. In this study, using expert expertise is preferred for the Mamdani-type fuzzy inference method in the rule-based fuzzy logic model. The type Mamdani consists of the following processes. The input variables are fuzzified to establish over membership functions to fit each of the fuzzy sets. Next, it uses a fuzzy 'AND' or 'OR' operator to combine the inputs to provide a single number. Next,

the weight of the rule is set before the consequence for every rule that is being applied. It combines and evaluates all the fuzzy rules. The outputs are aggregated by methods of aggregation, including maximum, probabilistic, and sum (simply the sum of the output set for each rule). Therefore, each rule's outputs are combined into a fuzzy collection that needs defuzzification [42]. The last step is defuzzification, which converts the fuzzy results to crisp output values. Some of the defuzzification methods are maximum mean (MM), centroid, maximum smallest (MS), and maximum largest (ML).

4.2 Artificial neural network

The NN can be described as a computational method whose processing is close to the behaviour of biological neurons. Also, it can be defined as a mathematical proof of the neural architecture of the individuals [43]. It is trained by the use of data, so restrictive assumptions are not mandatory in the model design process. It detects complex non-linear structures between variables depending on an independent [44]. It can be extended to the problems where the input–output relationship is ambiguous or unknown. MLP, whose general structure is shown in Fig. 5b, uses feed-forward architecture on multiple layers and is the most widely used network. An MLP is composed of three layers of input, hidden, and output. The input layer receives input data features and distributes them to the hidden layer. The hidden layer contains neurons and transforms the input into the form that can be interpreted by the output layer. The output layer also contains neurons and yields the final outputs. The optimal NN structure is usually established after trial and errors [45]. After training and testing using the data set, the model structure that provides the smallest error is selected. It is retrained until the expected level of precision has been achieved. The NNs as supervised and unsupervised networks are split into two classes, competitive layers and self-organising maps, which are trained to allow the network to continually adjust the new inputs. At the same time, the supervised networks are trained by using data to generate required input outputs. After training and testing using the data set, the model structure that provides the smallest error is selected. It is retrained until the expected level of precision has been achieved.

The NNs as supervised and unsupervised networks are split into two classes, competitive layers and self-organising maps, which are trained to allow the network to continually adjust the new inputs. At the same time, the supervised networks are trained by using data to generate required input outputs. These networks are the feed-forward networks (feed-forward-backpropagation cascade-forward backpropagation, perceptron etc.), radial base networks (generalised regression and probabilistic NNs), and dynamic networks (Elman, Hop field, non-linear self-regressive, etc.). Elman is using feed-forward backpropagation and cascade-forward backpropagation networks. Levenberg–Marquardt is one of the quickest and most effective training methods and is ideal for small and medium-sized networks training [46].

4.3 Adaptive neuro-fuzzy inference system

ANFIS combines NN and FISs 'advantages. Therefore, it has rapid learning ability, the ability to seize a process's non-linear structure, the ability to adapt, and does not require expert knowledge. The ANFIS has been successfully implemented in a variety of fields to a wide range of problems [47]. Besides, ANFIS can effectively solve any type of complex and non-linear problems by incorporating the advantages of NN and fuzzy logic. By using fuzzy methods, it blends numerical and linguistic information. This also uses the data classification capability and pattern recognition capabilities of the ANN. Furthermore, the ANFIS causes fewer memorisation errors and is more observable to the user than the ANN. ANFIS is essentially the fuzzy modelling based on rules. Fuzzy rules are established over the process of training [48]. The training is carried out with the use of a data set. The ANFIS designs an FIS, and the membership function parameters are formed based on the training data. The Sugeno-type FIS is used in the ANFIS model as the data set is used, and the ANFIS architecture is shown in Fig. 5c, where x and y as inputs. The

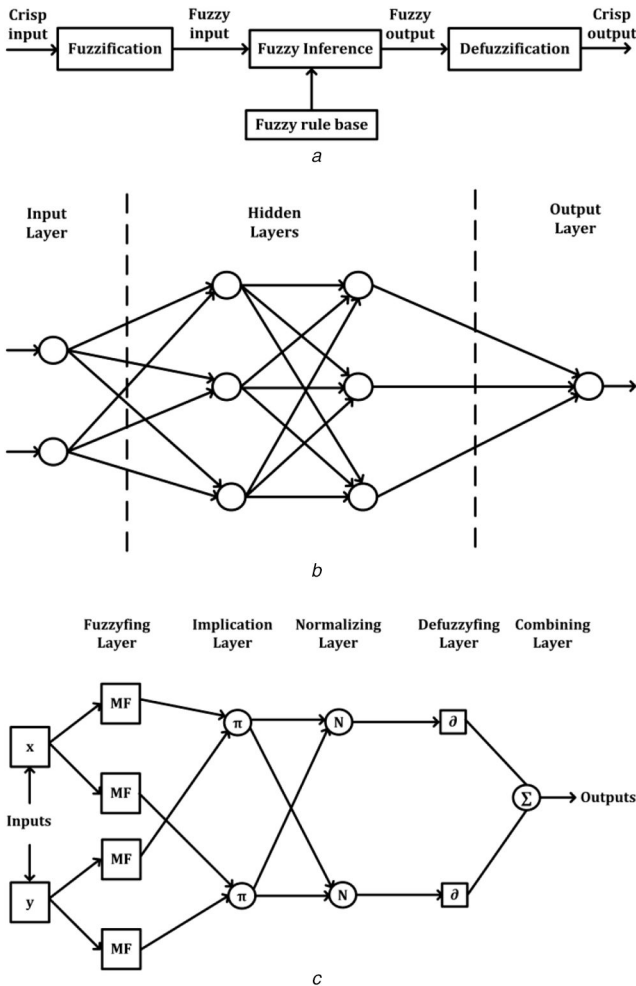


Fig. 5 Overall configuration of the applied different controllers
 (a) Fuzzy logic system, (b) MLP NN architecture, (c) The architecture of the ANFIS model with two inputs, one output, and two rules

ANFIS architecture consists of five layers; the first layer or fuzzifying layer; each neuron is an adaptive node consisting of premise parameters. Neurons indicate the product of inputs as in the second layer, known as the implication layer. While in the third layer or normalising layer, each neuron is fixed. In the fourth layer (de-fuzzifying layer), each neuron is also an adaptive one consisting of consequence parameters. Finally, the combining layer contains a single neuron that adds up all the inputs. The following section shows the implementation of the proposed algorithms. In general, estimating the calculation procedures requires the accurate data of AC and DC voltages along the pipeline. These data are generally derived from field measurements or simulations results. In practice, the AC and DC voltages is changing with time since it is affected by the changes of the soil constituents, operating temperature, and line currents. To overcome these variations, the proposed control system is developed to construct the relationship between AC and DC voltages under different conditions and then take suitable action. However, the influencing factors on AC and DC voltages are complex; forming the relationship between AC and DC voltages is still challenging. This work attempts to develop a suitable control system to compensate the DC voltage or mitigate the AC voltage.

5 Implementation of the proposed algorithms

Generally, the promotion of the efficacy of the CP system along the pipeline represents the challenge due to the DC CP potentials depend on several various factors such as soil properties, operating temperature, and weather conditions. This study attempts to overcome these factors to predict accuracy CP performance. Therefore, the rules of the controller are the most vital to present the relationship between variations input and outputs. This section

describes the different controllers of the local control system, which distributes at five points on the pipeline. Various controllers are then implemented to preserve the CP potential within reasonable limits, to reduce the induced voltage to a minimal value. Firstly, each controller requires to construct the relationship between the induced AC and DC voltages and then calculate its response to adjustments in the operating conditions of the pipeline. The model takes the variable parameters (i.e. induced AC and DC voltage) as input to the controller. For improving the CP performance, dual-input and a triple-output system have been established. The input variables are V_{AC} and V_{DC} , and the outputs are α_{KOH_i} , α_{CR_i} , and D_{st} . In this study, the expected value of V_{AC} ranges between 0 and 100 V, which denotes the value of the induced AC voltage. V_{DC} denotes the effectiveness of the CP potential. For the FLC, V_{AC} is classified into four ranges: low (L), medium (M), high (H), and very high (VH). V_{DC} is classified into five ranges: very low (VL), low (L), medium (M), high (H), and very high (VH) (see Fig. 6a). Moreover, the value of α_{KOH_i} ranges from 0° to 180° , which denotes the firing angle to KOH-PC's thyristor. Also, the value of α_{CR_i} ranges from 0° to 180° , which denotes the firing angle to the controlled rectifier. D_{st} denotes the status of the CP potential on the pipeline, and the value is an integer which ranges from 0 to 1. Besides, α_{KOH_i} is classified into three ranges: low firing (LF), medium firing (MF), and high firing (HF). α_{CR_i} is classified into five ranges: very low firing (VLF), low firing (LF), medium firing (MF), high firing (HF), and very high firing (VHF). D_{st} is classified into three ranges: low (L), medium (M), and high (H) (see Fig. 6b). For compensating the CP potential along the overall pipeline, five-input and a single-output fuzzy logic system have been established. The input variables are DC voltage state from each local FLC (D_{st}), and the output is the firing angles to two ICCP stations at the pipeline's terminals (α_{MCR_i}). For simplicity, the membership functions represent single input from five-inputs, in addition to a single-output. D_{st} denotes the status of the CP potential on the pipeline, as shown in Fig. 6c. Besides, an approach using an ANN is proposed to control the induced voltage produced on the pipeline and use it as an alternative source for improving the CP performance. The multilayer feed-forward ANN with the error backpropagation training method is employed. The input to the local ANN controller is the induced AC voltage and DC voltage as well as the output is the firing angle to KOH-PC's thyristor, the firing angle to the controlled rectifier, and the status of the CP potential on the pipeline. Besides, the input to the central ANN controller is the DC voltage status from each local ANN controller as well as the output of the central ANN controller is the firing angles to the main ICCP station. After experimenting with different training functions, the most appropriate training function is chosen for the problem. The number of hidden layers and neurons is determined through trial and error.

The proposed NN is feed-forward backpropagation, the number of the inputs to the local controller is 2 with 20 neurons, and the training algorithm is Levenberg–Marquardt. Besides, the number of inputs to the main controller is 5 with 20 neurons. The ANFIS developed in this study is an approximate fuzzy model with Sugeno-type based on Matlab. The subtractive clustering is used in the ANFIS models to produce FIS because the accuracy of the prediction obtained is higher than the grid partitioning. For induced AC voltage and CP against DC voltage, three membership functions are formed for each input variable. The hybrid method of optimisation is used for FIS training. Thus, for accurate tests, the number of epochs, which are 1000, is set. The parameters and features of the ANFIS models for subtractive clustering are given in Table 1. Besides, Table 2 shows the parameters for DC voltage state from each local ANFIS, and the output is the firing angles to two ICCP stations at the pipeline's terminals (α_{MCR_i}).

6 Results and discussions

Basically, the studied pipeline is considered an extension of the previous research paper, which was discussed in [34]. This pipeline is owned by Fayoum Gas Company, Egypt. In this paper, a

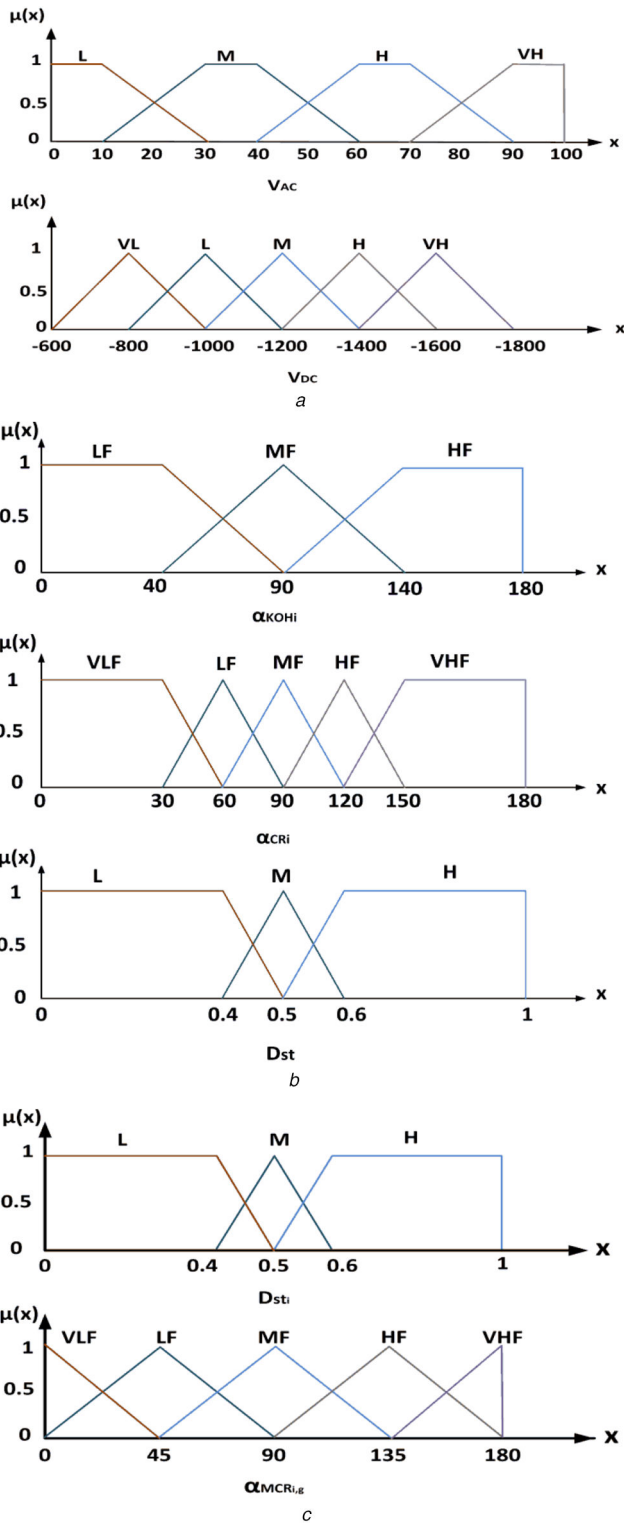


Fig. 6 Fuzzy sets for input and output parameters to fuzzy controller (a) Fuzzy sets for input parameters; V_{AC} , and V_{DC} , (b) Fuzzy sets for output parameters; α_{KOHI} , α_{CRI} , and D_{St} , (c) The optimised membership functions for the main fuzzy logic system

complementary analysis of either the induced AC voltage produced on the pipeline or the CP performance with a mitigation unit is introduced. A real case study of the Fayoum gas pipeline is studied. This pipeline has a 72 km length, which is parallel or crossing the three transmission lines (El-Kurimate-Cairo TL, Samaloute-Cairo TL, and Dimo-6th of October TL), as shown in Fig. 7a. Two of them carry a voltage of 500 kV and the last carries voltage of 220 kV. The towers of 500 kV TL have three-phase power circuits with two earth cable, in addition to the tower of 220 kV has two three-phase power circuits with one earth cable. Besides, the El-

Table 2 Properties of the proposed ANFIS models

Parameter	Description/value	Main ICCP stations
fuzzy inference system structure	Sugeno	Sugeno
optimisation method for training FIS	subtractive clustering	subtractive clustering
range of influence	0.87	0.87
squash factor	1.1	1.1
accept ratio	0.5	0.5
reject ratio	0.1	0.1
input number	2	5
output number	1	1
number of input membership functions	3,3	3,3,3,3
optimisation methods	hybrid	hybrid
training epoch numbers	1000	1000

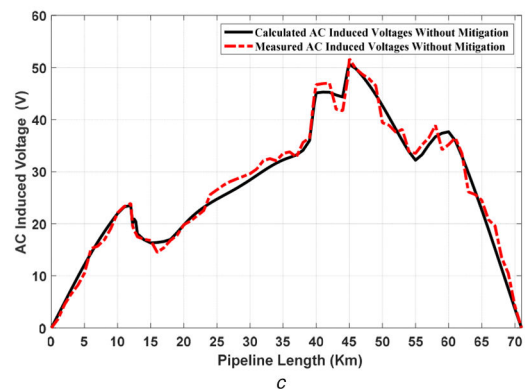
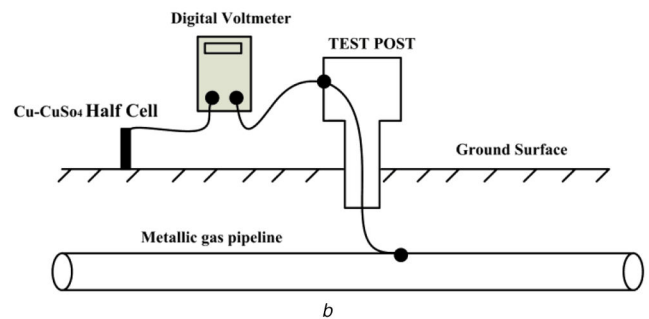
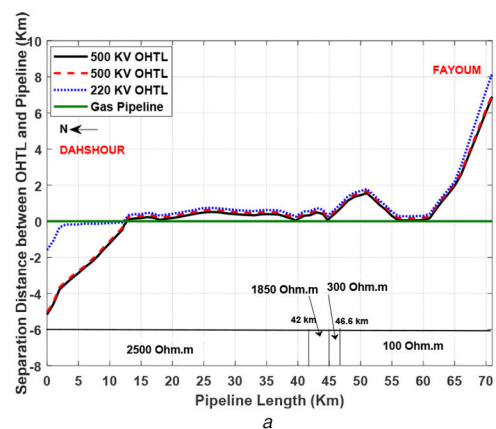


Fig. 7 Illustration of the study layout and induced voltage measurement (a) Fayoum gas co. pipeline- three power lines layout, (b) Experimental procedure to measure of induced AC voltage, (c) A comparison between the measured and the calculated induced AC voltage

Kurimate-Cairo transmission line has a length of 124 km with 575 MVA rated power, as well as the Samaloute-Cairo transmission

line, which has 1000 MVA rated power with 209 km. The last line is the Dimo-6th of October transmission line, while each circuit carries 158 MVA rated power. The specification data of these transmission lines, illustrated in Table 3, are taken from [49]. Besides, the study pipeline has a diameter of 0.4064 m, which coats by high-density polyethylene, where the thickness of the coating layer is 4 mm with resistance $10^6 \Omega/m^2$. Also, it is buried at a depth of 1.5 m with the soil resistivity varies from 2500 to 100 Ω m along with the pipeline layout.

In this study, the measurements of induced AC voltage is performed using a digital AC voltmeter, which is inserted between the pipeline and Cu-CuSO₄ portable electrode, as shown in Fig. 7b. The equivalent circuit of the pipeline is presented as shown in Fig. 1. The parameters of this circuit are calculated by MATLAB code, then the obtained results for the induced AC voltage are conducted to SIMULINK/MATLAB software. To validate the accuracy of the pipeline model, the calculated results are compared with real measurements. It is observed that a good agreement between the measured and calculated results is achieved. However, there are small divergences between them due to the complexity in measuring the accurate data of operating conditions of the transmission line and the surrounding environment of the pipeline as shown in Fig. 7c.

Fig. 8a depicts the profile of the induced AC voltage with and without KOH-PCs. It is observed that the induced voltage has a maximum value at some points. These points are 12.75, 18, 39.7, 44.8, and 58 km, which have 20.43, 17, 43.12, 49.79, and 35.93 V, respectively, as in Table 4. This indicates that the possibility of pipeline corrosion increases. Therefore, the induced voltage must be reduced to a safe limit (15 V) to avoid AC corrosion. This can be achieved by inserting KOH-PCs along the pipeline at the lowest separation distance between the transmission line and pipeline. After placing the different models of KOH-PCs on the pipeline, it can be noted that the AC induced voltage is reduced below the threshold value (15 V). After installing the KOH-PCs at the high voltage points, it is noticed that at point 54 km along the length of the pipeline, the induced voltages have maximum values that equal 14.32 and 14.5 V in case of using the PC-25 and PC-50, respectively.

On the other hand, after inserting the KOH-PCs for the pipeline, the DC voltage of CP is slightly decreased along the pipeline length. Consequently, the DC voltage may be significantly influenced, especially by installing the PC-50, which introduces an easier bridge to the soil for the current. Fig. 8b shows the DC CP

Table 3 Technical details of transmission lines [49]

Parameter	Value	
rated power, MVA	575	158
line to line voltage, kV	500	220
power lines length, km	124	90
tower circuits number	1	2
phase conductors number	3	2
the diameter of the conductor, mm	30.6	27
the conductors spacing, cm	47	30
the span of towers, m	400	360
conductor vertical height at the tower, m	19.1	15.7
overhead earth cables number	2	1
overhead earth cable height, m	30	41.8
overhead earth cable diameter, mm	11.2	13.6

Table 4 Induced AC voltage calculations using different KOH-PCs with different controllers

Point, km	PC-25			PC-50		
	ANN	FLC	ANFIS	ANN	FLC	ANFIS
12.75	2.83	1.761	1.233	1.33	0.793	0.52
18.00	2.98	1.695	1.186	1.32	0.965	0.63
39.70	3.29	2.54	1.778	1.539	1.178	0.767
44.80	4.02	1.544	1.15	2.35	0.944	0.611
58.00	5.82	3.027	2.12	5.54	2.641	1.716

voltage along the pipeline without and with KOH-PCs under different KOH plates. It is noticed that the minimum DC voltage occurs in the middle of the pipeline due to the longest distance from the main ICCP stations. The calculated values of the DC voltage at the middle pipeline are -0.767, -1.374, and -1.445 V for PC-50, PC-25, and without mitigation units, respectively. These values represent the minimum DC voltage along the pipeline. From this figure, it is noted that the discharging of the direct current to the soil will gradually increase if the KOH-PC plate's numbers are increased. Consequently, the DC voltage in the case of using PC-50 is the most critical compared to PC-25 due to the increase of the plate number in polarisation cells, which causes the increase of the electrical paths to the soil.

Therefore, it is necessary to implement different controllers system to control both the AC and DC voltages. As a result, the proposed model is based on the utilisation of the dissipated induced voltage into the soil to guarantee better CP performance. This proposed model is based on maintaining the DC voltage within allowable limits with saving in the energy demand from both the main ICCP at both pipeline's terminals. Therefore, the different controllers are used to tune and utilise the induced AC voltage in improving the DC voltage after inserting the mitigation units. Firstly, the performance of the proposed model is assessed by two criteria. Two criteria are used to judge the different controllers against each other, which are the annual saving energy (SE_{year}) and annual discharged energy (DE_{year}). Subsequently, the performance

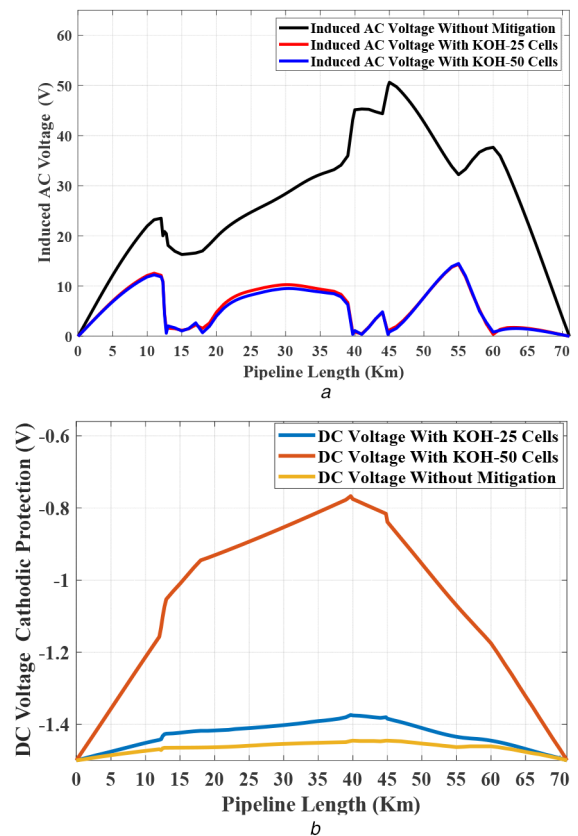


Fig. 8 AC and DC voltage calculation at various conditions

(a) The calculated induced AC voltage, (b) The DC CP voltage along the pipeline without and with KOH-PCs for different plates [25]

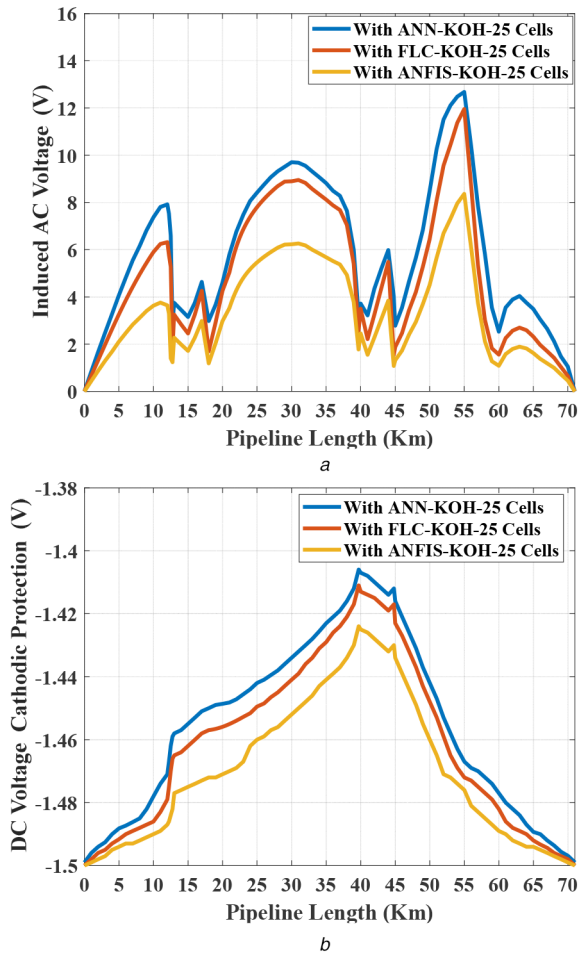


Fig. 9 Induced AC voltage and DC CP voltage along the pipeline in case of PC-25 with different controllers
(a) Calculated pipeline induced voltage, (b) Calculated DC voltage

of the ANN and fuzzy controllers, as well as the performance of the ANFIS controller to achieve complete CP under the same system conditions are recorded. Figs. 9a and b show the profile of the induced AC voltage and DC voltage in case of using PC-25 with different controllers, respectively.

As shown in two figures, an ANN controller gives reasonable results in which the mitigated induced voltage is significantly decreased from 14.32 to 12.68 V at 55 km, as well as the DC voltage improves from -1.374 to -1.406 V at 39.7 km. From these figures, it is noted that the performance of the model using the ANFIS controller is more effective than the performance accomplished using the FLC system, in which the mitigated AC voltage calculated values are 8.3664 and 11.952 V at 54 km, respectively compared to 14.32 V without the controller. Moreover, the DC voltage improves from -1.374 to -1.411 V and -1.424 V in the case of FLC and ANFIS, respectively, at 39.7 km.

Therefore, we can conclude that the response of the ANFIS controller to compensate DC voltage and mitigate the induced voltage is faster compared to the others controllers. Therefore, the ANFIS controller is the most efficient control method between the three suggested controller, where it achieves sufficient mitigation and reasonably CP performance under different KOH-PCs' models. Figs. 10a and b show the induced AC voltage using the PC-50 is more than that of the PC-25. At the same time, the DC CP performance is better than that without a controller. This means that the proposed controller constitutes an important role in the reduction of the induced voltage and the improvement of CP performance in the pipeline. As shown in two figures, the ANN controller improves the DC voltage from -0.767 to -0.87 V at PC-50. Besides, the improvement of the CP performance is evaluated during using FLC, and ANFIS, which improves the DC voltage from -0.767 to -0.956 V, and -1.096 V, respectively. Also, the mitigated induced AC voltage with ANN, FLC, and

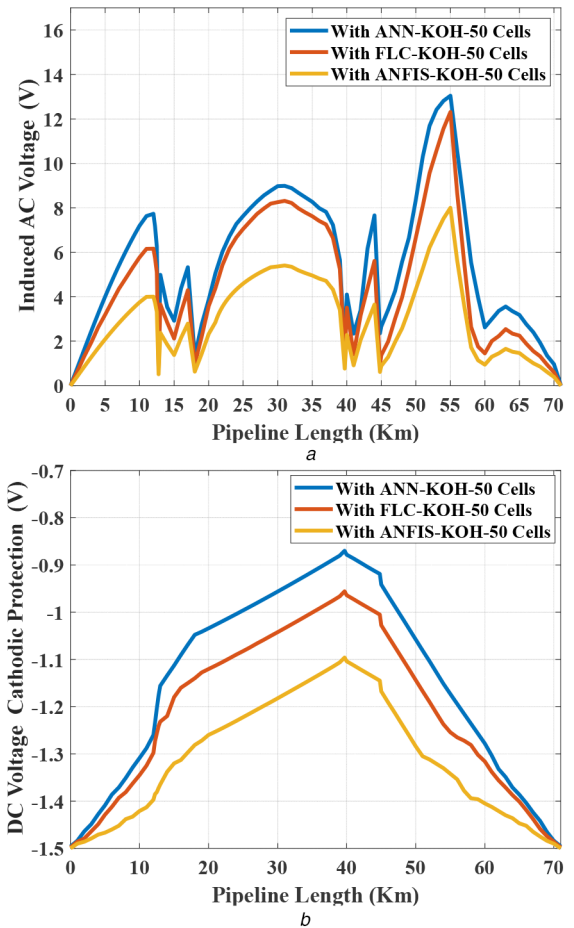


Fig. 10 Induced AC voltage and DC CP voltage along the pipeline in case of PC-50 with different controllers
(a) Calculated pipeline induced voltage, (b) Calculated DC voltage

ANFIS are 13.044, 12.31, and 8.0015 V. The above analysis indicates that the performance of CP is greatly improved by implementing the ANFIS controller. Moreover, the ability of ANFIS in achieving two criteria is better than those of FLC and ANN. Therefore, it can also be used ANFIS Controller to solve the problem of AC interference. From the previous figures, it is concluded that the mitigation of the induced voltage with the ANFIS controller is more than that of other controllers in different KOH-PC models, in addition to the overall performance of CP along the pipeline will improve. The proposed model results prove that the ANFIS controller gives the best performance in achieving two purposes; the first aim is the mitigation of the induced voltage, and the second aim is the improvement of DC potential.

Table 4 shows the comprehensive comparisons for the highest induced AC voltage points under different controllers. Furthermore, to evaluate the precision of the proposed model, its results are developed with various controllers. As shown in Table 4, the obtained results indicate higher accuracy of the ANFIS controller over other controllers. It is observed that the ANFIS controller with PC-50 gives the promise results in the reduction of the induced voltage compared to other controllers. The reduction in induced voltage with PC-50 is more than that with PC-25. To sum up, the proposed model using ANFIS successfully achieves the global reduction of the induced voltage in different KOH-PCs' models compared to other controllers'. From the author's point of view, it can be noted from the above-mentioned results that the ANFIS controller is a considerable control method, which provides a highly efficient saving in power energy extracted from ICCP's stations. Also, as seen in Table 5, one can note that the ANFIS controller achieved the best CP performance, whereas the other controller gives a reasonable result. Besides, the results indicate that the proposed model achieves superior CP performance. The compensation in DC voltage obtained by the ANFIS controller is more than that obtained using ANN and FLC controllers. As seen

Table 5 DC voltage calculations using PC-25 with different controllers

Point, km	PC-25			
	Without controller	ANN	FLC	ANFIS
12.75	-1.427	-1.459	-1.465	-1.482
18.00	-1.418	-1.45	-1.458	-1.472
39.70	-1.374	-1.406	-1.411	-1.424
44.80	-1.38	-1.412	-1.421	-1.43
58.00	-1.44	-1.472	-1.477	-1.485

Table 6 DC voltage calculations using PC-50 with different controllers

Point, km	PC-50			
	Without controller	ANN	FLC	ANFIS
12.75	-1.073	-1.176	-1.241	-1.372
18.00	-0.945	-1.048	-1.142	-1.281
39.70	-0.767	-0.87	-0.956	-1.096
44.80	-0.816	-0.919	-1.005	-1.145
58.00	-1.133	-1.236	-1.281	-1.394

Table 7 Annual saving and dissipating energy with different controllers

Controller	PC-25		PC-50	
	SE _{year} , MWh	DE _{year} , MWh	SE _{year} , MWh	DE _{year} , MWh
ANN	3.804	07.623	2.124	13.690
FLC	4.212	07.215	3.897	11.917
ANFIS	4.487	06.940	6.783	09.031

in Table 6, one can note that the PC-50 is no longer risky for CP performance. The CP voltage values along the pipeline will exceed the minimum allowable limit of CP voltage (-0.85 VDC) is defined by the NACE standard.

Table 7 shows the comparative analysis of the three controllers in terms of energy-saving and discharging per year to demonstrate the performance of the proposed model. The delivered energy per annum from the main ICCP units to the pipeline is about 30 MWh. While, the total discharged energy per year is 11.427 and 15.814 MWh using PC-25 and PC-50, respectively. The saved energy in the case of ANFIS is greater than that obtained using the other controllers. From these tables, it is noticed that the response of the different controllers to compensate for the DC voltage reduction is reasonable. Besides, in the analysis of the results, one can note a significant improvement in overall CP performance in three controllers. Consequently, the AC interference problem associated with the effect of the mitigation unit on the CP performance is eliminated.

To sum up, the proposed model using ANFIS successfully achieves the global purpose, which includes the improvement of CP DC voltage and the reduction of the induced AC voltage along the pipeline to protect the pipeline against AC corrosion. Also, in comparison to the different controller's results, the proposed model scheme is more effective in the improvement of DC voltage and the utilisation of the induced AC voltage on the pipeline. From the simulation results, it is confirmed that the proposed ANFIS is efficient in accurately improving the DC CP potential and also mitigating the induced voltage on pipelines.

7 Conclusion and extensions

This paper discusses the interference between the transmission lines and neighbouring metallic pipelines, as well as describes the mechanisms that cause the inducing of the AC voltage on these pipes. In normal conditions, the AC induced voltage is studied due to the inductive coupling between the power lines and pipelines. A complete Simulink model has been represented for the pipeline and the coupling mechanism. Comprehensive comparisons have been

introduced between the calculated and the measured values of the AC induced voltage. Besides, this comparison shows the approximated identity between the calculated and the measured. This step should follow to validate the accuracy of the Simulink model. Then the discharging of the AC induced voltage has been studied based on the electrical model of the different types of KOH-PCs. In parallel with these cells, controlled rectifier circuits have been installed. The main purpose of these circuits is to convert the AC voltage, which causes pipeline corrosion, to a suitable DC voltage. An electronic switch will install between the pipeline and the KOH-PC, which connects in parallel with a controlled rectifier circuit. Three intelligent controllers are implemented to control either the discharged energy to the soil or the injected current into the pipeline. These controllers are ANN, FLC, and ANFIS, which are introduced in this paper. To discriminate the performance of these controllers, KPIs are used. Both SE_{year} and DE_{year} are considered the main KPIs that should be optimally satisfied to reduce the delivered energy from the utility grid and maximise the discharged energy to the soil. SE_{year} represents the delivered energy from the distributed KOH-PCs to the pipeline or the saved energy that should deliver from the main ICCP units to the pipelines. In other words, if SE_{year} increases, the delivered energy from KOH-PCs will increase, and also the saved energy from the main ICCP units will increase. Therefore, this KPI is selected to judge which controller has the best performance. It is found that ANFIS gives the highest SE_{year}, so it is considered the most intelligent controller to achieve the main objective to protect the pipeline. Therefore, it is essential to improve the proposed model in the future by widely applying this model under different fault conditions of the transmission line as well as with different seasons. Besides, the proposed model will be extended in the future using an optimised metaheuristic-based controller to utilise for preventing the AC corrosion. This paper states the base for advanced future work, where the KOH-PC may replace by the solid-state polarisation cells. Additionally, the communication between the different controllers should be studied to determine the most proper communication and its generation; 4G or 5G.

8 References

- [1] Lucca, G.: 'Different approaches in calculating AC inductive interference from power lines on pipelines', *IET Sci. Meas. Technol.*, 2018, **12**, pp. 802–806
- [2] Micu, D., Christoforidis, G., Czumbil, L.: 'AC interference on pipelines due to double circuit power lines: a detailed study', *Electr. Power Syst. Res.*, 2013, **103**, pp. 1–8
- [3] Ouadah, M., Touhami, O.: 'Method for diagnosis of the effect of AC on the X-70 pipeline due to an inductive coupling caused by HVPL', *IET Sci. Meas. Technol.*, 2017, **11**, (6), pp. 766–772
- [4] Lu, M., Xie, Y., Zhu, W., et al.: 'Determination of the magnetic permeability, electrical conductivity, and thickness of ferrite metallic plates using a multi-frequency electromagnetic sensing system', *IEEE Trans. Ind. Inf.*, 2018, **15**, pp. 4111–4119
- [5] Peabody, A.W.: 'Control of pipeline corrosion'. In: Bianchetti, RL (ed): (NACE International the corrosion society, Houston, Texas, 2001), p. 49
- [6] NACE Standard RP0169: 'Control of external corrosion on underground or submerged metallic piping systems'. NACE International, 2007
- [7] DS 91. 'Standard for the Selection and Design of Cathodic Protection (CP) Systems'. 2017
- [8] Yuji, H., Fumio, K., Yasuo, N.: 'New CP criteria for elimination of the risks of AC corrosion and over-protection on cathodically protected pipelines'. Corrosion, Houston, USA, 2002, Paper No. 02111
- [9] Aghay, K., Amer, H., Abdulrahim, S.: 'Prediction of metallic conductor voltage owing to electromagnetic coupling via a hybrid ANFIS and backtracking search algorithm', *Energies*, 2019, **12**, (19), p. 3651
- [10] Roya, N., Bhardwaj, A.: 'Effect of heterogeneities on pitting potential of line pipe steels: an adaptive neuro-fuzzy approach', *Corrosion Science*, 2018, **133**, (1), pp. 327–335
- [11] Ahmed, K.: 'Location estimation of coating defects and mitigation of induced AC voltages along buried gas pipeline', *IET Sci. Meas. Technol.*, 2018, **12**, (2), pp. 209–217
- [12] Biezma, M., Agudo, S.: 'A fuzzy logic method: predicting pipeline external corrosion rate', *Int. J. Press. Vessels Pip.*, 2018, **163**, pp. 55–62
- [13] Kim, Y., Seok, S.: 'Optimizing anode location in impressed current cathodic protection system to minimize underwater electric field using multiple linear regression analysis and artificial neural network methods', *Eng. Anal. Bound. Elem.*, 2018, **96**, pp. 84–93
- [14] Dipak, J., Barnali, B.: 'Novel type-2 fuzzy logic approach for inference of corrosion failure likelihood of oil and gas pipeline industry', *Eng. Fail. Anal.*, 2017, **80**, pp. 299–311

- [15] Victoria, B., Diego, A., Gonzalo, B.: 'A fuzzy logic method: predicting pipeline external corrosion rate', *Int. J. Press. Vessels Pip.*, 2018, **163**, pp. 55–62
- [16] Qi, Z., Wei, W.: 'Estimation of corrosion failure likelihood of oil and gas pipeline based on fuzzy logic approach', *Eng. Fail. Anal.*, 2016, **70**, pp. 48–55
- [17] Pavanaditya, B., Yakesh, B., Jayapriya, J.: 'Risk evaluation of oil and natural gas pipelines due to natural hazards using fuzzy fault tree analysis', *J. Nat. Gas Sci. Eng.*, 2019, **66**, pp. 284–292
- [18] Priyanka, E.B., Maheswari, C., Thangavel, S.: 'Online monitoring and control of flow rate in oil pipelines transportation system by using PLC based fuzzy-PID controller', *Flow Meas. Instrum.*, 2018, **62**, pp. 144–151
- [19] Levente, C., Dan, M., Denisa, S., *et al.*: 'A neural network approach for the inductive coupling between overhead power lines and nearby metallic pipelines'. Proc. of the 2016 Int. Symp. on Fundamentals of Electrical Engineering (ISFEE), Bucharest, Romania, 30 June–2 July 2016, pp. 1–6
- [20] Wu, W.: 'Oil and gas pipeline risk assessment model by fuzzy inference systems and artificial neural network'. MSc thesis, University of Regina, Faculty of Graduate Studies and Research, 2015
- [21] Mohammed, S., Ahmed, S.: 'Artificial neural network models for predicting condition of offshore oil and gas pipelines', *Autom. Constr.*, 2014, **45**, pp. 50–65
- [22] Ahmed, B., Risza, R.: 'Estimation of failure probability using fault tree analysis and fuzzy logic for CO₂ transmission', *Int. J. Environ. Sci. Develop.*, 2014, **5**, (1), pp. 26–30
- [23] Ali, J., Abdolreza, C., Siamak, Y., *et al.*: 'Developing a new fuzzy inference system for pipeline risk assessment', *J. Loss Prev. Process Ind.*, 2013, **26**, (1), pp. 197–208
- [24] Dan, M., Levente, C., Georgios, C.: 'Neural networks applied in electromagnetic interference problems', *Revue Roumaine des Sci. Techn.*, 2012, **57**, (2), pp. 162–171
- [25] Al-Badi, A., Ellithy, K., Al-Alawi, S.: 'Prediction of voltages on mitigated pipelines paralleling electric transmission lines using ANN', *Int. J. Comput. Appl.*, 2010, **32**, (1), pp. 15–22
- [26] Al-Badi, A., Ellithy, K., Al-Alawi, S.: 'Prediction of voltages on mitigated pipelines paralleling electric transmission lines using an artificial neural network', *J. Corros. Sci. Eng.*, 2007, **10**, pp. 24–28
- [27] Xiaobin, L., Wei, L., Jingyi, X.: 'Intelligent diagnosis of natural gas pipeline defects using improved flower pollination algorithm and artificial neural network', *J. Clean Prod.*, 2020, **264**, p. 121655
- [28] Chinedu, I.: 'Corrosion defect modelling of aged pipelines with a feed-forward multi-layer neural network for leak and burst failure estimation', *Eng. Fail. Anal.*, 2020, **110**, p. 104397
- [29] Kai, W., Lei, H., Jing, L., *et al.*: 'An optimization of artificial neural network modeling methodology for the reliability assessment of corroding natural gas pipelines', *J. Loss Prevention Process Ind.*, 2019, **60**, pp. 1–8
- [30] Qi, L., Yuan, H., Li, L.: 'Calculation of interference voltage on the nearby underground metal pipeline due to the grounding fault on overhead transmission lines', *IEEE Trans. Electromagn. Compat.*, 2013, **55**, (5), pp. 965–974
- [31] Australian/New Zealand Standard.: 'Electrical hazards on metallic pipelines'. (AS/NZS 4853, 2000)
- [32] Hui, Z., George, K.: 'Effect of various parameters on the inductive induced voltage and current on pipelines', *IEEE Trans. Power Deliv. Ariz. State Univ.*, 2011, pp. 1–7, doi: 10.1109/PES.2011.6038882
- [33] Nasser, T.: 'Power systems modelling and fault analysis theory and practice' (Elsevier Ltd, USA, 2008)
- [34] Mostafa, A., Mohamed, M., Abdel salam, H., *et al.*: 'Modeling of the KOH-polarization cells for mitigating the induced AC voltage in the metallic pipelines', *Heliyon*, 2020, **6**, (3), pp. 1–10
- [35] CP-3.: 'Cathodic Protection Technologist course manual'. NACE. International Standard, 2005
- [36] Marcassoli, P., Bonetti, A., Lazzari, L., *et al.*: 'Modeling of potential distribution of subsea pipeline under cathodic protection by finite element method', *Mater. Corros.*, 2015, **66**, (7), pp. 619–626
- [37] Montoya, R., Nagel, V., Galván, J., *et al.*: 'Influence of irregularities in the electrolyte on the cathodic protection of steel: a numerical and experimental study', *Mater. Corros.*, 2016, **64**, (12), pp. 1055–1065
- [38] Baeckmann, W., Schwenk, W., Prinz, W.: 'Handbook of cathodic corrosion protection' (Chemical Industry Press, Germany, 2005, 3rd edn.)
- [39] Guofu, Q., Bingbing, G., Jinping, O.: 'Numerical optimization of an impressed current cathodic protection system for reinforced concrete structures', *Constr. Build. Mater.*, 2016, **119**, pp. 260–267
- [40] Lotfi, Z.: 'Fuzzy logic – a personal perspective', *Fuzzy Sets Syst.*, 2015, **281**, pp. 4–20
- [41] Singh, H., Gupta, M., Meitzler, T.: 'Real-life applications of fuzzy logic', *Adv. Fuzzy Syst.*, 2013, **2013**, (2013), pp. 1–3
- [42] Michael, N.: 'Artificial intelligence: a guide to intelligent systems' (Pearson Education, London, UK, 2011)
- [43] Filippo, A., Alberto, L.: 'Artificial neural networks in medical diagnosis', *J. Appl. Biomed.*, 2013, **11**, pp. 47–58
- [44] Ciobanu, D., Vasilescu, M.: 'Advantages and disadvantages of using neural networks for predictions', *Ovidius Univ. Ann., Series Econ. Sci.*, 2013, **13**, (1), pp. 444–449
- [45] Mukesh, T., Chandranath, C.: 'Development of an accurate and reliable hourly flood forecasting model using wavelet-bootstrap-ANN (WBANN) hybrid approach', *J. Hydrol.*, 2010, **394**, (3), pp. 458–470
- [46] Hao, Y., Bogdan, W.: 'Levenberg–Marquardt training in intelligent systems' (CRC Press, Boca Raton, FL, USA, 2011), pp. 1–16
- [47] Barak, S., Sadegh, S.: 'Forecasting energy consumption using ensemble ARIMA–ANFIS hybrid algorithm', *Int. J. Electr. Power Energy Syst.*, 2016, **82**, pp. 92–104
- [48] Mohammad, G., Milad, A., Amir, M.: 'Application of ANFIS soft computing technique in modeling the CO₂ capture with MEA, DEA, and TEA aqueous solutions', *Int. J. Greenhouse Gas Control*, 2016, **49**, pp. 47–54
- [49] Gouda, O., Zain, A., Al-Gabalawy, M.: 'Effect of electromagnetic field of overhead transmission lines on the metallic gas pipelines', *Electr. Power Syst. Res.*, 2013, **103**, (129), pp. 129–136